MOLECULAR AND CELLULAR BIOLOGY, Mar. 1997, p. 1254–1263 Vol. 17, No. 3
0270-7306/97/$04.00+0

The Structure of Heterochromatic DNA Is Altered in Polyploid Cells of *Drosophila melanogaster*

ROBERT L. GLASER,[1,2]* THOMAS J. LEACH,[1] AND STEPHANIE E. OSTROWSKI[2]

Laboratory of Developmental Genetics, Wadsworth Center, New York State Department of Health,[1] *and Department of Biomedical Sciences, University at Albany, State University of New York,*[2] *Albany, New York 12201-2002*

Received 8 July 1996/Returned for modification 9 September 1996/Accepted 10 December 1996

DNA sequences within heterochromatin are often selectively underrepresented during development of polyploid chromosomes, and DNA molecules of altered structure are predicted to form as a consequence of the underrepresentation process. We have identified heterochromatic DNAs of altered structure within sequences that are underrepresented in polyploid cells of *Drosophila melanogaster*. Specifically, restriction fragments that extend into centric heterochromatin of the minichromosome *Dp(1;f)1187* are shortened in polyploid cells of both the ovary and salivary gland but not in the predominantly diploid cells of the embryo or larval imaginal discs and brains. Shortened DNA molecules were also identified within heterochromatic sequences of chromosome III. These results suggest that the structure of heterochromatic DNA is altered as a general consequence of polyploid chromosome formation and that the shortened molecules identified form as a consequence of heterochromatic underrepresentation. Finally, alteration of heterochromatic DNA structure on *Dp(1;f)1187* was not correlated with changes in the variegated expression of the *yellow* gene located on the minichromosome.

Heterochromatic chromosomal domains, such as those that include the centromere and telomeres, are defined by a variety of cytological and genetic criteria. They are persistently condensed throughout the cell cycle, replicate late in S phase, are enriched in highly repetitive satellite sequences, and suppress the expression of adjacent euchromatic genes in a process known as position-effect variegation (PEV) (for general reviews, see references 11, 21, 23, 24, 32, and 53 and references therein). Recent progress has been made in our understanding of heterochromatin on a number of fronts including the large-scale sequence structure of heterochromatic domains (30, 33), the role of heterochromatin domains in chromosome pairing and segregation (10, 25, 38), the protein components of heterochromatin structure (2, 7, 14, 28, 51), and the mechanism of PEV (8, 9, 21, 42).

Heterochromatic domains can also undergo dynamic change during development. A classic example is the heterochromatization of the inactivated X chromosome in female mammals (35). DNA sequences within heterochromatin can also be actively eliminated during somatic development, as occurs in a variety of organisms including species of protozoans, nematodes, crustaceans, insects, and fish (3, 15, 36, 39, 40, 48). In fact, heterochromatic DNAs are disproportionately or exclusively targeted in most, if not all, cases of chromosome diminution.

Heterochromatic sequences can also be selectively underrepresented during the development of polyploid chromosomes (reviewed in reference 47). This phenomenon is particularly dramatic during the development of polyploid chromosomes in dipteran insects such as *Drosophila melanogaster*, where the copy number of a given satellite sequence may be reduced many hundred-fold relative to euchromatic DNA (13, 41). While underrepresentation is widely assumed to result from selective underreplication of heterochromatic sequences (29), no direct evidence substantiating this model has been reported (16, 27). More recently, alternative models have been proposed that include mechanisms of DNA elimination (16, 27, 45, 46) and copy-choice replication (21). Despite an extensive literature describing the phenomenon of heterochromatic underrepresentation, the molecular mechanism that underlies this property of heterochromatin remains to be determined.

We have addressed the phenomenon of heterochromatic underrepresentation by using the *Dp(1;f)1187* minichromosome of *Drosophila melanogaster* (*Dp1187*). *Dp1187* is a small (1,300-kb) derivative of the *In(1)sc*^{8} chromosome (27, 31). It has all the principal structural features of higher eukaryotic chromosomes, including distinct euchromatic and heterochromatic domains (see Fig. 1) (30), and demonstrates normal meiotic and mitotic segregation functions (27, 38). A restriction map encompassing both euchromatic and heterochromatic domains of the chromosome has been constructed, facilitating its molecular analysis (30). *Dp1187* has been used extensively to address questions of chromosome structure, especially as relates to heterochromatin (16, 17, 26, 27, 37, 38, 55). In particular, studies on heterochromatic underrepresentation involving *Dp1187* prompted a reappraisal of underreplication as the mechanism of underrepresentation (16, 27, 46).

DNA molecules of altered structure are predicted to form between regions of fully represented euchromatic and underrepresented heterochromatic DNA. Identification of such molecules and determination of their structure would provide significant insight into the mechanism of underrepresentation. Evidence for such molecules has been provided by earlier analyses of *Dp1187* in which structurally altered derivatives of the *Dp1187* chromosome were identified in polyploid cells (45, 46). In this report, we extend these earlier observations by using the *Dp1187* minichromosome to characterize underrepresentation in polyploid cells of *Drosophila* and identify heterochromatic molecules of altered structure within underrepresented sequences. The characteristics of these structurally altered molecules are consistent with those expected to arise from heterochromatic underrepresentation.

* Corresponding author. Mailing address: Wadsworth Center, NYSDOH, P.O. Box 22002, Albany, NY 12201-2002. Phone: (518) 473-4201. Fax: (518) 474-3181. E-mail: robert.glaser@wadsworth.org.

MATERIALS AND METHODS

***Drosophila* strains.** Information about *Drosophila* genes and nomenclature may be found in reference 31. Flies were maintained at 22°C and 50% relative humidity. Samples of ovary and imaginal-disc-plus-brain DNA used for the quantitative analysis illustrated in Fig. 2 and the two-dimensional analysis illustrated in Fig. 3 were isolated from female progeny of the cross *X, y* × *X, y/Y*; *Dp(1;f)1187*, y^+. This cross ensured that a single *Dp(1;f)1187* chromosome was present in virtually all *yellow*$^+$ offspring and that the *Dp/X* hybridization ratio in y^+ females was 0.5. Embryos for the same analyses were collected from the *X, y*; *Dp(1;f)1187*, y^+ female progeny of this cross that had mated randomly with both *X, y/Y* and *X, y/Y*; *Dp(1;f)1187*, y^+ male sibs. The average *Dp/X* hybridization ratio for a population of these embryos, assuming random mating, is predicted to be 0.5.

Samples of embryo, ovary, and salivary gland DNA used for the analysis illustrated in Fig. 4A were isolated from strain *Df(1)sc*^{8}, *y*; *Dp(1;f)1187*, y^+. Individual animals in this strain had either one (36%), two (57%), or three (7%) copies of the *Dp(1;f)1187* chromosome (unpublished observation). Samples of embryo, ovary, and salivary gland DNA used for the analysis illustrated in Fig. 4B were isolated from strain CH(3)336, which is homozygous for a P-element insertion into region h54-57 of chromosome III (56). Salivary glands used for both analyses illustrated in Fig. 4 were isolated from female larvae. Ovary DNA used for the analysis illustrated in Fig. 5B was isolated from adult females of genotype *X^X, y*/O; *Dp1187*, y^+, which were obtained from the cross *X^X, y*/O × *X^Y, Df(1)259 l(1)J1 y*/O; *Dp1187*, y^+, and from adult females of genotype *X^X, y/Y*; *Dp1187*, y^+, which were obtained from the cross *X^X, y*/O × *X, y/Y*; *Dp1187*, y^+.

Preparation and digestion of DNA in agarose inserts. Agarose-embedded ovary and imaginal-disc-plus-brain DNA were prepared as described previously (17). Briefly, ovaries from adult females and imaginal-disc-plus-brain complexes from third-instar larval females were dissected in saline and held on ice. The tissues were then gently homogenized, and the homogenate was mixed with molten agarose and pipetted into insert molds. The inserts were treated with proteinase K and rinsed extensively before digestion with restriction enzymes. For agarose-embedded embryo DNA, embryos were collected on grape-agar plates, dechorionated in 50% Clorox bleach, and homogenized and the DNA was prepared as described for ovaries and imaginal-disc-plus-brain complexes. Agarose-embedded salivary gland DNA was prepared as described previously (27). Briefly, salivary glands were dissected in saline and homogenized and nuclei were isolated by centrifugation through sucrose. The nuclei were then prepared in agarose as described for ovaries and imaginal-disc-plus-brain complexes. Tissues were dissected from a large number of animals at one time, pooled, and prepared as described above. Individual samples contained DNA from 1 to 10 pairs of ovaries, 1 to 8 μl of dechorionated embryos, 20 pairs of salivary glands, or 6 larval imaginal-disc-plus-brain complexes. Agarose-embedded DNA was digested overnight with appropriate restriction enzymes by using the manufacturer's buffers in which bovine serum albumin was added to 100 μg/ml and RNase A was added to 10 μg/ml. The restriction enzymes used for individual experiments are described in the appropriate figure legends.

Electrophoresis and DNA hybridization. Fractionation of DNA by conventional or contour-clamped homogeneous electric field (CHEF) electrophoresis (5) was performed as described previously (17). A variety of pulsing regimens were used on the CHEF gels depending on the needs of a given experiment (described in the figure legends). After electrophoresis, DNA was analyzed by either Southern blot, in-gel, or two-dimensional agarose gel hybridization. Southern blotting was performed by standard methods (43; see also reference 17), and subsequent hybridizations were done by the procedures of Church and Gilbert (6). In-gel hybridizations were performed as described previously (17). Briefly, after electrophoresis, the agarose gels were dried to completion in a 65°C gravity convection oven. The dried gels were rehydrated, and the DNA was denatured and neutralized before hybridizing directly to the gels by the procedures of Church and Gilbert (6). Two-dimensional agarose gel hybridizations were performed as described previously (17). The procedure is described briefly in Results.

Subclones of *X* chromosome genomic DNA used as hybridization probes have all been described previously (17) and include a 1.75-kb *Hin*dIII-*Eco*RI fragment from position −103 (HR1.75), a 3.5-kb *Eco*RI fragment from position −54 (R3.5), a 2.6-kb *Ase*I-*Hin*dIII fragment or 3.7-kb *Xba*I-*Hin*dIII fragment from the *sc*^{8} breakpoint (AH2.6; XH3.7), and a 0.8-kb *Bgl*II-*Pst*I fragment from position −1.7 (BP0.8). The probe used for the euchromatic control hybridization illustrated in Fig. 4A was a 7-kb *Hin*dIII fragment from the *rosy* locus. The hybridization probe used to identify restriction fragments flanking the P-element insertion in strain CH(3)336 (Fig. 4B) was a 3-kb *Pst*I fragment encompassing the bacterial *lacZ* gene.

Probes were made from DNA fragments isolated in low-melting-temperature agarose and labeled with ^{32}P by random priming (12) to specific activities of approximately 10^9 cpm/μg. After hybridization, filters and gels were exposed to Kodak XAR-5 film at −80°C with intensifying screens for qualitative analysis. For quantitative analysis, the blots and gels were analyzed with a Molecular Dynamics PhosphorImager and ImageQuant software.

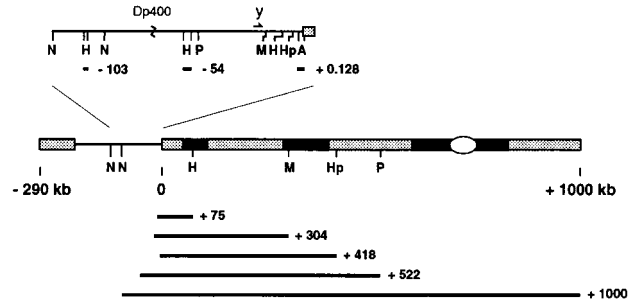

FIG. 1. Structure of *Dp(1;f)1187*. A map of the complete *Dp1187* minichromosome is shown with relevant restriction fragments indicated. The coordinate system used (in kilobases) is indicated, where 0 kb is defined as the position of the *sc*^{8} rearrangement junction. Sequences to the right, or proximal, of the *sc*^{8} breakpoint extend into heterochromatic sequences near the centromere and are denoted by positive values. Sequences to the left, or distal, of the *sc*^{8} breakpoint are denoted by negative values. Euchromatic sequences are shown as a line, and heterochromatic sequences are shown as a gray bar. Three "islands" of complex heterochromatic sequences are shown in black (30). The approximate location of the centromere is indicated by the open oval (38). Above the complete map is an expanded view of the first 125 kb of euchromatic sequences distal to the *sc*^{8} junction. Positions of the *yellow* gene and the deletion endpoint of *Dp400* are indicated. The restriction fragments analyzed in this report are shown as black lines in their appropriate locations below the complete and the expanded maps. Each fragment is denoted by its proximal-most endpoint, which is shown to the right. The restriction sites that generate each fragment are shown on the map. A, *Ase*I; H, *Hin*dIII; Hp, *Hpa*I; M, *Mlu*I; N, *Not*I; P, *Pme*I.

RESULTS

Heterochromatic restriction fragments isolated from polyploid cells demonstrate persistent copy number reductions. The structure of heterochromatic DNA was studied by using the 1.3 Mb *Dp(1;f)1187* minichromosome of *Drosophila*. The general structure of *Dp1187* is illustrated in Fig. 1, with restriction sites and restriction fragments pertinent to this study shown. The derivation of *Dp1187* from the *In(1)sc*^{8} chromosome and detailed restriction mapping of *Dp1187* have been described previously (30). *Dp1187* contains 1 Mb of centromeric heterochromatic DNA, which consists of interspersed blocks of satellite DNA and "islands" of more complex sequences (Fig. 1) (30). The *Dp1187* chromosome is segregated normally during meiosis and mitosis and has been used to study numerous aspects of chromosome structure and function (see Introduction).

In polyploid chromosomes subject to heterochromatic underrepresentation, DNA molecules of altered structure are predicted to form between regions of fully represented euchromatic and underrepresented heterochromatic sequences (29). Previous experiments that directly tested this prediction, however, failed to identify DNA molecules of altered structure in a region of the *Dp1187* chromosome suggested to contain a steep copy number gradient (16). Interpretation of this result, however, is complicated by the fact that heterochromatic restriction fragments of *Dp1187* can appear severely underrepresented in vitro despite being fully represented in vivo as a consequence of the selective inability of *Dp1187* heterochromatic DNA to transfer efficiently during Southern blotting (17). This unusual property of these heterochromatic DNAs accounts for some, but not all, underrepresentation of *Dp1187*.

In light of these observations, we first sought to identify copy number reductions of *Dp1187* sequences caused by true in vivo underrepresentation. Evidence for such a copy number reduction was observed previously while characterizing the Southern blot transfer inhibition phenomenon (17). Specifically, a restriction fragment spanning the *sc*^{8} junction of *Dp1187* and

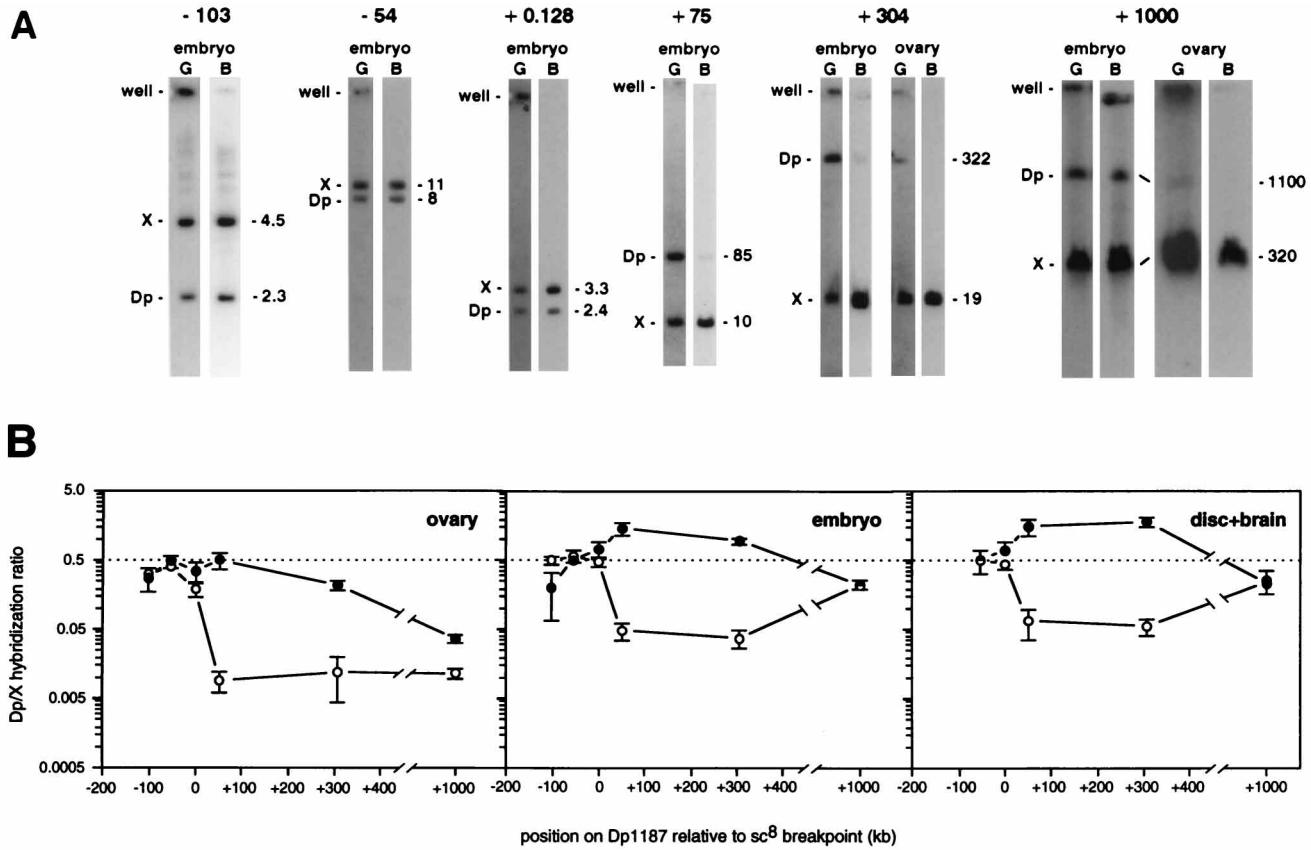

FIG. 2. Quantitative Southern blot and in-gel hybridization analysis of *Dp(1;f)1187* reveals persistent underrepresentation in a polyploid tissue. (A) In-gel (lanes G) and Southern blot (lanes B) hybridizations are illustrated for six different digests of embryo DNA and two different digests of ovary DNA. The number above each set of panels indicates the proximal endpoint of the *Dp1187* restriction fragment analyzed (Fig. 1). The *Dp1187*-specific (Dp) and *X*-specific (X) bands are indicated, and their sizes (in kilobase pairs) are shown. Samples for −103 were digested with *Hin*dIII, fractionated by conventional electrophoresis, and probed with HR1.75. Samples for −54 were digested with *Hin*dIII, fractionated by conventional electrophoresis, and probed with R3.5. Samples for +0.128 were digested with *Ase*I, fractionated by conventional electrophoresis, and probed with AH2.6. Samples for +75 were digested with *Hin*dIII, fractionated by CHEF electrophoresis for 12 h with a 10-s switch time, and probed with AH2.6. Samples for +304 were digested with *Mlu*I, fractionated by CHEF electrophoresis for 13 h with a linearly ramped switch time of 10 to 90 s, and probed with AH2.6. Samples for +1,000 were digested with *Not*I, fractionated by CHEF electrophoresis for 13 h with a linearly ramped switch time of 10 to 150 s, and probed with AH2.6. The higher-molecular-weight bands in −103 are not a result of partial digestion by *Hin*dIII but are due to cross-hybridization of the probe with heterogeneous high-molecular-weight molecules in this digest. The hybridization signal observed in the wells of in-gel hybridizations is an artifact of the procedure and does not necessarily indicate a legitimate hybridization signal. Autoradiographs of Southern blot and in-gel analyses of −103, −54, +0.128 and +75 digests of ovary DNA have been reported previously (17). (B) Southern blot and in-gel hybridization analysis of DNA isolated from whole adult ovaries, 0- to 12-h embryos, and larval imaginal-disc-plus-brain complexes were quantitated with storage-phosphorimaging plates. The mean and standard error calculated from three to seven independent measurements for each digest assayed by Southern blot (open circles) or in-gel (filled circles) hybridizations is shown. Ratios are plotted on a log scale versus the position of the proximal endpoint of the *Dp1187* restriction fragment assayed. The expected *Dp1187*-to-*X* hybridization ratio was 0.5 in DNA from all three tissues (see Materials and Methods) and is shown as a horizontal dashed line.

extending 1,000 kb into heterochromatic sequences was underrepresented in DNA isolated from polyploid ovarian nurse and follicle cells of the ovary. Underrepresentation of this fragment probably reflected true in vivo copy number loss and was not an artifact of Southern blot transfer inhibition because the fragment was also underrepresented on in-gel hybridizations, which are done directly to dried-down gels without Southern blot transfer.

To characterize *Dp1187* underrepresentation in ovaries and establish that the underrepresentation observed reflected true in vivo copy number reductions, *Dp1187* DNA isolated from ovaries was analyzed by Southern blot and in-gel hybridization and compared to *Dp1187* DNA isolated from predominantly diploid tissues (Fig. 2). In diploid tissues, heterochromatic underrepresentation is not expected to occur. The predominantly diploid tissues analyzed included 0- to 12-h embryos and third-instar larval imaginal-disc-plus-brain complexes. Relative to ovaries, 0- to 12-h embryos are enriched for diploid cells. By 12 h of embryonic development, only yolk, salivary gland, gut, and malpighian tubule cells have initiated polyploid development, and except for yolk nuclei, these cells have completed only a single polyploid S phase (44). Larval imaginal-disc-plus-brain preparations contain predominantly diploid cells with some polyploid cells contributed by the central nervous system (50).

Six different restriction fragments of *Dp1187* were analyzed. Two fragments were located entirely within euchromatin at positions −103 and −54, and four fragments spanned the sc^8 euchromatic-heterochromatic junction extending into heterochromatic sequences to kb +0.128, +75, +304 and +1000 (Fig. 1; restriction fragments are designated by the position of their heterochromatic endpoints). The copy number of each fragment was determined by measuring the hybridization level to the *Dp1187*-specific restriction fragment relative to the hybridization level in the same sample to a wholly euchromatic restriction fragment from the normal *X* chromosome that was

identified by the same probe (Fig. 2) (see Materials and Methods). The flies analyzed had the genotype *X/X*; *Dp1187* such that a *Dp/X* hybridization ratio of 0.5 is predicted for *Dp1187* fragments that are fully represented. A sample of Southern blot and in-gel hybridization results are illustrated in Fig. 2A, and the complete quantitative analysis for all three tissues is illustrated in Fig. 2B.

Overall, much of the behavior of *Dp1187* in all three tissues was similar (Fig. 2B). Euchromatic restriction fragments −103 and −54 and the +0.128 restriction fragment measured by both Southern blot and in-gel analysis were at or close to the expected copy number for fully represented euchromatic DNAs. The +75 heterochromatic restriction fragment in all three tissues, on the other hand, was subject to significant Southern blot transfer inhibition. This was evidenced by the severe underrepresentation of this fragment measured by Southern blot hybridization (10- to 100-fold) but normal or near-normal levels of representation measured by in-gel hybridization (Fig. 2B).

Most relevant to this report was the behavior of restriction fragments extending +304 and +1,000 kb into heterochromatic sequences. In ovary DNA, these fragments were still significantly underrepresented when assayed by in-gel hybridization (2- and 14-fold, respectively [Fig. 2]), suggesting that the heterochromatic sequences on these fragments are underrepresented in vivo. In embryo and disc-plus-brain DNA, only the +1,000 fragment was underrepresented by in-gel hybridization and only twofold below predicted levels (Fig. 2). Surprisingly, the +75 and +304 fragments in embryo and disc-plus-brain DNA appeared overrepresented on in-gel hybridizations (Fig. 2). Subsequent analysis indicated that this overrepresentation, however, does not reflect actual in vivo increases in *Dp1187* copy number (see the two-dimensional analysis discussed below). The reason that elevated hybridization ratios were observed for only these two fragments and no other DNAs, including euchromatic restriction fragments or lambda DNA controls, is not known (Fig. 2; data not shown).

Heterochromatic underrepresentation is associated with DNA molecules of altered structure. *Dp1187* molecules of altered structure must be present in ovary DNA if the copy number reductions suggested by the in-gel analysis reflect true in vivo underrepresentation. Specifically, discontinuities in the linear structure of DNA must occur within the heterochromatic sequences of the +304 and +1,000 restriction fragments to account for the fact that the euchromatic portions of these molecules are fully represented while the full-length molecules are underrepresented (Fig. 1 and 2B). Furthermore, any DNA molecules of altered structure that are formed should be detectable by hybridization since the restriction fragments used as probe are located within fully represented euchromatic sequences. Despite these predictions, however, no hybridization signals indicative of *Dp1187*-specific molecules of altered structure were detected in the analysis illustrated in Fig. 2.

We considered whether detection of altered *Dp1187* molecules of reduced size may have been obstructed by hybridization signal to the *X* chromosome-derived euchromatic restriction fragment present in each sample (Fig. 2A). We suspected that such molecules might be present given the detection of shortened derivatives of the *Dp1187* chromosome in undigested ovary DNA reported previously (45, 46). To address this possibility, *Dp1187* DNA was analyzed by a two-dimensional agarose gel hybridization technique that physically separates all *Dp1187*-derived and *X*-derived DNAs in a single sample, allowing for their independent analysis without the complications of overlapping hybridization signals (Fig. 3) (17). Briefly, the two-dimensional gel technique involves fractionating genomic DNA on a first-dimension, pulsed-field gel like those illustrated in Fig. 2A. Then a lane of the first-dimension gel is excised, and DNA in the gel slice is digested in situ with a second enzyme, *Bgl*II. *Bgl*II cuts the *Dp1187* chromosome within euchromatic sequences at kb −3.2 and −1.7 and cuts the *X* chromosome at kb −3.2 and +0.6. The gel slice is then molded into a second agarose gel, and the double-digested DNA is fractionated by electrophoresis perpendicular to the direction used for the first-dimension gel. DNA separated in the second-dimension gel is then detected by conventional Southern blot hybridization. The positions of restriction fragments in the first-dimension gel slice are revealed by the positions of the *Bgl*II fragments in the second-dimension gel. The *X*-derived and *Dp1187*-derived *Bgl*II fragments identified by the probe are polymorphic in size, resulting in the physical separation of the *X*-specific and *Dp1187*-specific molecules into discrete lanes in the second-dimension gel. Finally, heterochromatic restriction fragments that transfer poorly during regular Southern blotting are more readily detected on the two-dimensional gels because the *Dp1187 Bgl*II fragment identified by the probe derives from wholly euchromatic sequences that transfer normally.

The two-dimensional gels revealed that the underrepresentation of full-length *Dp1187* molecules observed in ovary DNA was caused, at least in part, by the formation of structurally altered *Dp1187* molecules with significantly increased electrophoretic mobility, as if shortened in size (Fig. 3). Shortened *Dp1187* molecules were detected in +304, +418, +522, and +1,000 restriction digests of ovary DNA. Two distinct populations of shortened molecules were detected in uncut DNA (Fig. 3), a result that corroborates previous analyses of *Dp1187* chromosomes marked with P-element insertions in which two populations of shortened derivatives were also found in uncut ovary DNA (45, 46). Shortened *Dp1187* molecules were not detected in DNA isolated from embryos or imaginal-disc-plus-brain preparations (Fig. 3), consistent with the in-gel hybridization results indicating that substantial underrepresentation was associated only with polyploid ovary DNA (Fig. 2). In addition, shortened molecules were associated only with heterochromatic restrictions fragments of *Dp1187* and not with euchromatic fragments from the *X* chromosome (Fig. 3).

In the single-dimension analysis of the +1,000 digest, the *X*-derived DNA fragment prevented detection of shortened *Dp1187* molecules (Fig. 2A and 3). In the +304 digest, however, this was unlikely to be the case, given the difference in size between the *X* and *Dp1187* molecules (Fig. 2A and 3). The shortened *Dp1187* molecules in +304 digests could be detected on single-dimension gels, however, if the hybridization signal to the shortened molecules was increased by using pulsed-field gel electrophoresis parameters that compressed resolution in the 74-kb size range and by loading more DNA (data not shown).

On average, the shortened *Dp1187* molecules represented approximately 50% of the total *Dp1187*-derived hybridization signal measured in each of the +304, +418, +522, +1,000, and uncut samples (Fig. 3). Quantitatively, then, formation of the altered *Dp1187* molecules can account for the twofold underrepresentation observed for the +304 fragment measured by in-gel hybridization (Fig. 2). A 50% abundance of altered fragments, however, does not fully account for the 10-fold underrepresentation of the +1,000 fragment (Fig. 2B and 3). Hybridization to the full-length +1,000 fragment may have been disproportionately reduced because the +1,000 fragment was preferentially retained in the sample well during electrophoresis compared to the DNA molecules of altered structure that were smaller in size. This explanation would be consistent with

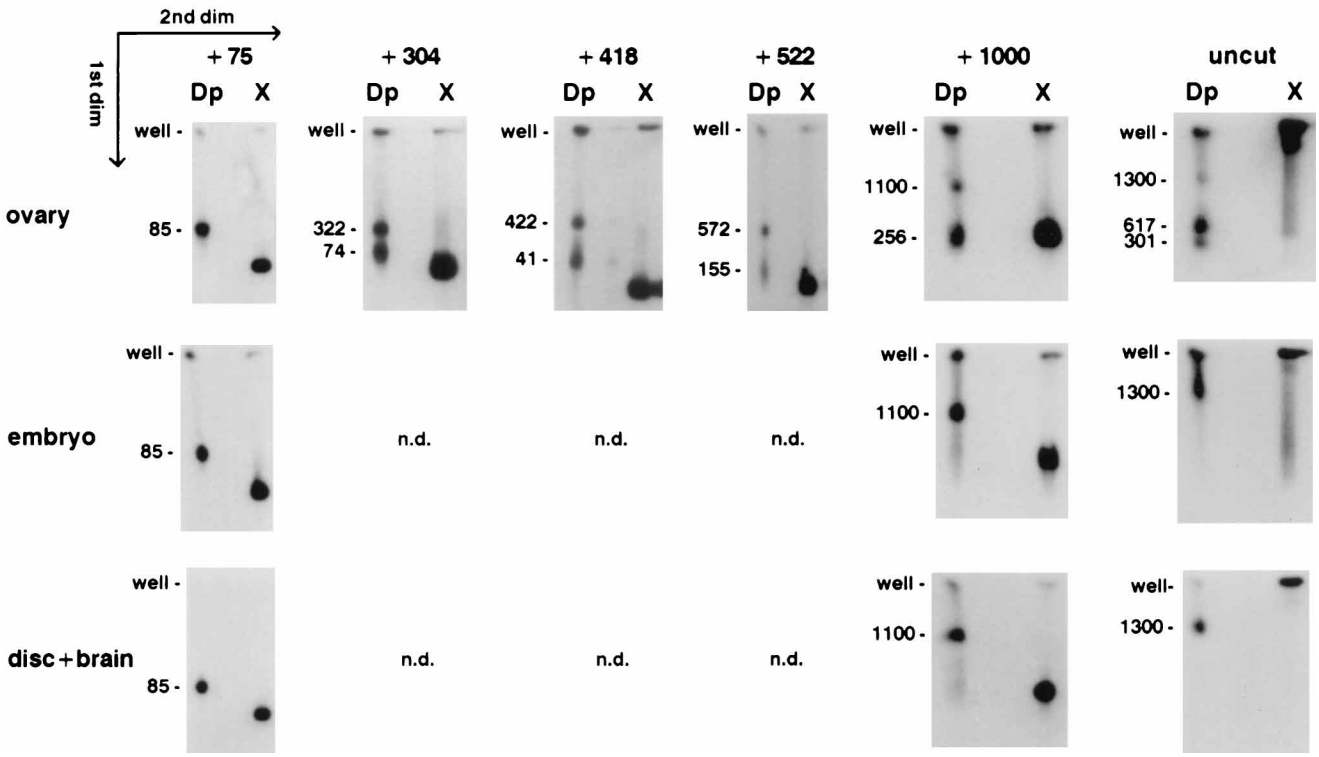

FIG. 3. Analysis of *Dp(1;f)1187* by two-dimensional agarose gel hybridization reveals shortened heterochromatic DNAs. DNA isolated from adult ovaries, 0- to 12-h embryos, and larval imaginal-disc-plus-brain complexes was digested with *Hin*dIII (+75), *Mlu*I (+304), *Hpa*I (+418), *Pme*I (+522), or *Not*I (+1,000) or left undigested (uncut) and fractionated on a first-dimension gel by CHEF electrophoresis with a linearly ramped switch time of 50 to 130 s for +75, +1,000 and uncut samples and 10 to 150 s for +304, +418, and +522 samples. Individual lanes from the first-dimension gel were excised, and the DNA was restricted in situ with *Bgl*II. The gel slice was then molded into a second agarose gel, and the double-digested DNA was fractionated in the second dimension by conventional electrophoresis. *Bgl*II sites are polymorphic between the *X* and *Dp1187* chromosomes, resulting in a discrete lane of 3.8-kb *X*-specific molecules (lanes X) and a discrete lane of 1.8 kb *Dp*-specific molecules (lanes Dp) in the second dimension. The direction of the first-dimension electrophoresis for each panel is from top to bottom, while the direction of the second-dimension electrophoresis is from left to right. Finally, the second-dimension gel was subject to Southern blot hybridization with probe BP0.8. The sizes (in kilobase pairs) of the full-length and shortened *Dp1187* molecules relative to the first-dimension electrophoresis are indicated. n.d., no data available.

the increased hybridization signal observed to the wells of +1,000 digests (Fig. 2A and 3 and data not shown). Finally, the twofold underrepresentation of the +1,000 fragment observed in embryo and disc-plus-brain DNA (Fig. 2B) can be accounted for by a heterogeneous background of *Dp1187*-specific hybridization observed in +1,000 digests of these samples (Fig. 3).

The two-dimensional analysis also revealed that the +75 restriction fragment of *Dp1187* is fully represented in all three tissues (Fig. 3). This observation corroborates the in-gel hybridization results, which also suggested that the +75 fragment is fully represented (Fig. 2B), and provides additional evidence that the underrepresentation of the +75 fragment observed on Southern blot hybridizations is an artifact of the inefficient transfer of *Dp1187* heterochromatic DNAs during Southern blotting (Fig. 2) (17). In addition, detection of the +75 fragment at the expected copy number on two-dimensional gels suggests that the overrepresentation of the +75 and +304 fragments observed in embryo and disc-plus-brain DNA by in-gel hybridization is unlikely to result from in vivo changes in *Dp1187* copy number (Fig. 2B).

Alteration of heterochromatic DNA structure occurs in two different types of polyploid cells. We wanted to accurately compare the altered heterochromatic DNAs of *Dp1187* isolated from different tissues. Such direct comparisons were technically difficult when two-dimensional gels were used, but altered heterochromatic DNAs could be visualized and directly compared on single-dimension Southern blots by using flies with a *Df(1)sc*^{8}; *Dp1187* genotype. In these flies, all euchromatic sequences distal of the *sc*^{8} breakpoint are unique to the *Dp1187* chromosome, and hybridizations can be done to *Dp1187*-derived molecules without interference from the *X* chromosome. Because *Dp1187* heterochromatic DNAs transfer poorly during standard Southern-blotting protocols (Fig. 2) (17), longer autoradiographic exposures were required to visualize *Dp1187* molecules. By using *Df(1)sc*^{8}; *Dp1187* flies, DNA was prepared from diploid-cell-enriched 0- to 12-h embryos, polyploid ovaries, and polytene salivary glands. Restriction fragments +75, +304, +418, and +1,000, along with uncut DNA, were analyzed by single-dimension Southern blot hybridization (Fig. 4A).

As anticipated, altered heterochromatic DNAs of increased electrophoretic mobility were observed on single-dimension gels of *Df(1)sc*^{8}; *Dp1187* DNA (Fig. 4A). Shortened molecules were observed in ovary DNA migrating at the same size as the molecules detected on two-dimensional gels, suggesting that the two techniques reveal the same population of altered *Dp1187* molecules (Fig. 3 and 4A). Most important, shortened molecules were also observed in DNA isolated from polytene salivary gland cells (Fig. 4A). For the +75, +304, and +418 digests, the altered heterochromatic DNAs from salivary glands were similar in size and relative abundance to the molecules observed in ovary. This observation suggests that formation of altered heterochromatic DNAs is a general conse-

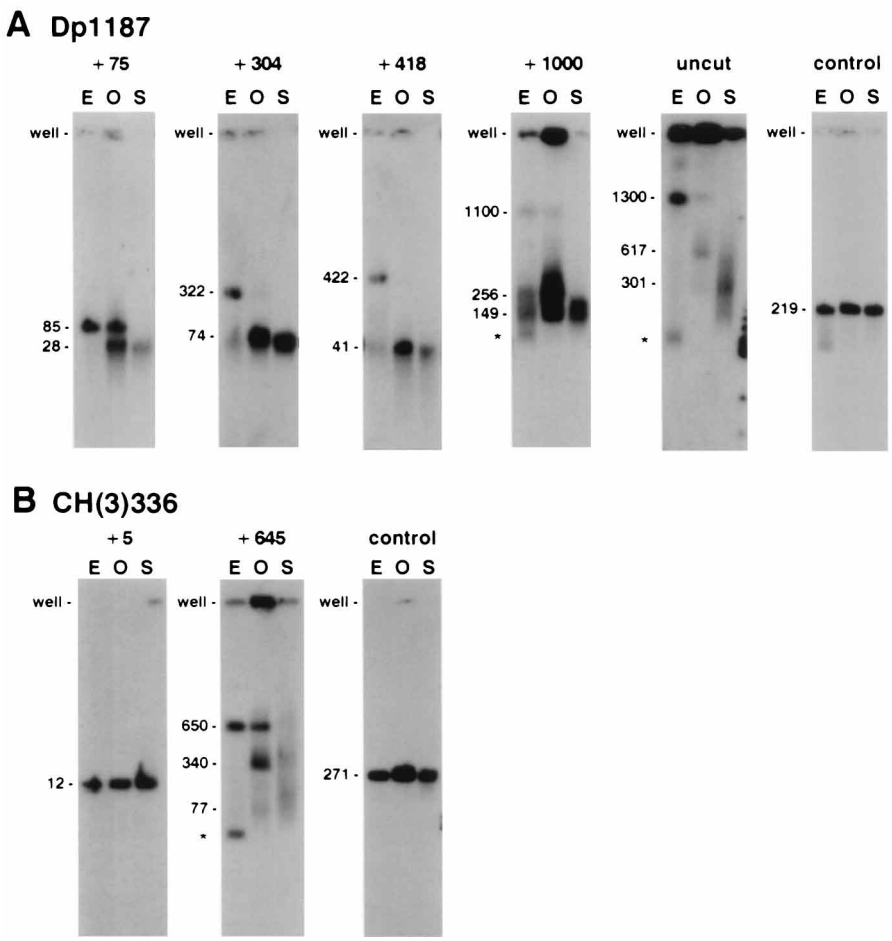

FIG. 4. The structure of heterochromatic DNA is altered in polyploid cells of both the ovary and salivary gland and within heterochromatic sequences of both the *Dp(1;f)1187* minichromosome and chromosome III. (A) *Dp1187* DNA from fly strain *Df(1)sc*^{8}; *Dp1187* was isolated from 0- to 12-h embryos (lanes E), adult ovaries (lanes O), and larval salivary glands (lanes S) and digested with *Hin*dIII (+75), *Mlu*I (+304), *Hpa*I (+418), or *Not*I (+1,000) or left undigested (uncut). The DNA was fractionated by CHEF electrophoresis with a linearly ramped switch time of 10 to 150 s and analyzed by Southern blot hybridization with probe AH2.6 or XH3.7. The control hybridization was to *Not*I-digested DNA with a probe to the euchromatic *rosy* locus. The sizes (in kilobase pairs) of full-length and shortened *Dp1187* molecules are indicated. A shortened heterochromatic molecule of 50 kb present only in embryo DNA is indicated by the asterisks. (B) DNA from fly strain CH(3)336, which has a P element inserted within chromosome III heterochromatin, was isolated from 0- to 12-h embryos (lanes E), adult ovaries (lanes O), and larval salivary glands (lanes S). The DNA was digested with *Xba*I (+5), or *Not*I (+645) and then fractionated and analyzed by Southern blot hybridization as described for panel A, except that the probe was to bacterial *lacZ* sequences contained on the P element. The control hybridization was to *Not*I-digested DNA with probe AH2.6, which, in strain CH(3)336, identifies only euchromatic sequences on the *X* chromosome. A shortened heterochromatic molecule of 22 kb present only in embryo DNA is indicated by an asterisk.

quence of polyploid chromosome formation rather than the product of a cell-type-specific process. Shortened *Dp1187* molecules were also detected in 0- to 12-h embryo DNA but were always present at reduced abundance relative to levels observed in either polyploid tissue (Fig. 4A). These DNAs may derive from the few cell types present in the embryo samples that initiate polyploidy by 12 h of development (44). Finally, shortened molecules were associated only with heterochromatic restriction fragments of *Dp1187* and not with control fragments from euchromatic regions of the genome (Fig. 4A).

Interestingly, the sizes of the shortened molecules observed in salivary gland DNA for the +1,000 and uncut samples were smaller, on average, than the comparable molecules in ovary DNA (Fig. 4A). In uncut samples, salivary gland DNA lacked the prominent band of 617-kb molecules and had more of the 301-kb and smaller molecules (Fig. 4A). In +1,000 samples, salivary gland DNA lacked the prominent band of 256-kb molecules. This difference might be a consequence of the greater severity of heterochromatic underrepresentation known to occur in salivary gland chromosomes compared to the chromosomes of ovarian nurse cells (18, 19). Alternatively, the shortened molecules may form in a qualitatively different way in the polytene chromosomes of the salivary gland and in the more diffuse polyploid chromosomes of the ovarian nurse and follicle cells.

The shortened *Dp1187* molecules appeared to transfer more efficiently than did the full-length molecules during Southern blotting of one-dimensional gels. This difference caused the shortened molecules to appear more abundant relative to full-length fragments on one-dimensional gels than on the two-dimensional gels (Fig. 3 and 4A). Perhaps the structural changes that create the shortened molecules remove sequences responsible for transfer inhibition (17). Although transferring poorly, full-length molecules were detectable in all ovary DNA samples if sufficiently long autoradiographic exposures were used (Fig. 4A and data not shown). In contrast, full-length molecules were never detected in salivary gland samples by any assay including one-dimensional, two-dimensional, and in-gel

hybridizations (Fig. 4A and data not shown). The absence of detectable full-length molecules in salivary gland DNA may reflect the severe heterochromatic underrepresentation that occurs in this tissue (13, 18, 19). Finally, the 28-kb shortened molecules detected in the +75 digest illustrated in Fig. 4A were not detected in the two-dimensional gel illustrated in Fig. 3 because the switching time used in the first-dimension pulsed-field gel electrophoresis did not resolve the shortened and full-length molecules.

Heterochromatic DNA of chromosome III is altered in structure. To determine if heterochromatic DNA elsewhere in the *Drosophila* genome is altered in polyploid chromosomes, restriction fragments extending into heterochromatic sequences of chromosomes II and III were analyzed. Entry into these regions of the genome was provided by P-element transposons inserted into heterochromatin (56). Six different chromosome II strains and five different chromosome III strains that each carry a single heterochromatic P-element insertion were analyzed. DNA was isolated from each strain, digested with a variety of eight-cutter restriction enzymes, and analyzed by single-dimension Southern blot hybridization. The P elements carry a bacterial *lacZ* gene that provides a unique-sequence probe, limiting hybridization to restriction fragments flanking each P-element insertion.

The structure of heterochromatic DNA flanking a P element inserted into region h54-57 of chromosome III [strain CH(3)336] was altered in polyploid tissues (Fig. 4B). Specifically, a restriction fragment extending 645 kb into heterochromatic sequences was shortened in ovary and salivary gland DNA. A fragment extending only 5 kb into flanking sequences was unaltered, consistent with an earlier analysis of these heterochromatic insertions (54), and control DNAs from euchromatic regions of the genome and present in the same samples were unaltered (Fig. 4B). Changes in the structure of the chromosome III heterochromatic DNA were similar in overall pattern to changes observed for fragments of *Dp1187* heterochromatic DNA, particularly comparing the +645 fragment of CH(3)336 and the *Dp1187* uncut sample (Fig. 4). Analysis of uncut DNA from strain CH(3)336 gave little or no detectable hybridization except to the sample wells (data not shown).

Detecting alterations in DNA structure within chromosome III heterochromatin demonstrates that the formation of shortened heterochromatic molecules is not a peculiarity of the *Dp1187* minichromosome or of *X* chromosome-derived heterochromatic sequences and that heterochromatic DNAs located in multiple regions of the *Drosophila* genome are altered in structure in polyploid cells. Detecting shortened heterochromatic DNAs in only 1 of 11 P-element strains may indicate that structural changes occur in a limited number of heterochromatic locations. Alternatively, most of the P elements may be inserted too far away from underrepresented regions of heterochromatin for structural rearrangements to be observed in flanking restriction fragments.

Finally, an unexpected phenomenon associated with heterochromatic DNA was revealed by the single-dimension Southern blot hybridization analysis. Shortened heterochromatic molecules unique to embryo DNA were observed. These molecules were detected in the +1,000 and uncut embryo samples of *Dp1187* and the +645 embryo sample of CH(3)336 (Fig. 4). In addition to their absence from ovary and salivary gland DNA, these molecules were absent from disc-plus-brain DNA (data not shown). These results suggest that heterochromatic DNA may be subject to structural changes that occur in cell types or during processes that are unique to embryonic development.

Alteration of heterochromatic DNA structure is not correlated with PEV. It has been proposed that the spread of heterochromatic underrepresentation into euchromatic sequences causes some instances of PEV (27). This proposal was based on a correlation that was observed between the underrepresentation of euchromatic sequences on the *Dp1187* chromosome and variegated expression of the *yellow* gene located within those sequences (27). *yellow* variegation has also been correlated with changes in the structure of *Dp1187* (45). Specifically, it was observed that terminal deletions of the *Dp1187* chromosome that remove a large amount of distal telomeric sequences cause both strong enhancement of *yellow* gene variegation (45, 49, 55) and changes to the structure of the shortened *Dp1187* molecules found in ovary DNA (45; also see below). If the observed changes in *Dp1187* structure are a consequence of heterochromatic underrepresentation, as has been proposed (45, 46; see above), this observation is consistent with a model in which underrepresentation can cause PEV.

In the experiments correlating *yellow* variegation with structural changes of *Dp1187*, uncut ovary DNA was analyzed (45). We wanted to know if the structure of the shortened *Dp1187* molecules detected in restriction enzyme-digested DNA, as illustrated in this report (Fig. 3 and 4A), would also be influenced by a PEV-enhancing terminal deletion. For example, if alterations of DNA structure spread toward and into euchromatic sequences near the sc^8 breakpoint leading to *yellow* variegation, one might expect to see a reduction in the size of shortened *Dp1187* molecules found in restriction enzyme-digested DNA. This prediction was tested by analyzing flies carrying either the *Dp1187* chromosome or *Dp400*, a *Dp1187* derivative lacking sequences distal to position −71 (Fig. 1) (55). This terminal deletion causes significantly increased *yellow* variegation with 70 to 80% $yellow^-$ triple-row bristles compared to 1 to 5% for *Dp1187* (55). This terminal deletion has also been shown to significantly alter the structure of shortened molecules observed in uncut ovary DNA (45; also see below).

DNA molecules of altered structure were revealed by two-dimensional electrophoresis, in uncut and restriction enzyme-digested ovary DNA from flies carrying *Dp1187* or *Dp400*. The results are illustrated in Fig. 5A. In *Dp1187* samples, the full-length and shortened molecules detected were the same as those illustrated in Fig. 3 and 4A. In *Dp400* samples, the sizes of the full-length molecules were consistent with those predicted for deletion of sequences distal to position −71 kb (Fig. 1 and 5A). The changes in the sizes of the shortened molecules detected in uncut and +1,000 samples of *Dp400*, however, are less easily accounted for by the terminal deletion. For example, in uncut DNA, the full-length *Dp400* molecule was 250 kb smaller than *Dp1187*, as expected, but the single population of 110-kb molecules observed in *Dp400* DNA appeared to be 507 and 191 kb smaller than the two populations of shortened molecules observed in *Dp1187* DNA (Fig. 5A). Likewise, in the +1,000 digest, the full-length *Dp400* molecule was 50 kb smaller than the *Dp1187* molecule, again as expected, while the single population of 110-kb molecules in *Dp400* DNA appears to be 146 kb smaller than the shortened molecules in *Dp1187* DNA. These disproportionate reductions in the sizes of the shortened DNA molecules in uncut and +1,000 digests of *Dp400* correlate with the observed increase in *yellow* variegation and are consistent with the earlier analysis of this chromosome (45).

Changes to DNA structure that correlate with changes in *yellow* variegation, however, were less evident in +304 and +418 digests. In fact, no consistent differences between *Dp1187* and *Dp400* were observed in the sizes or amounts of the short-

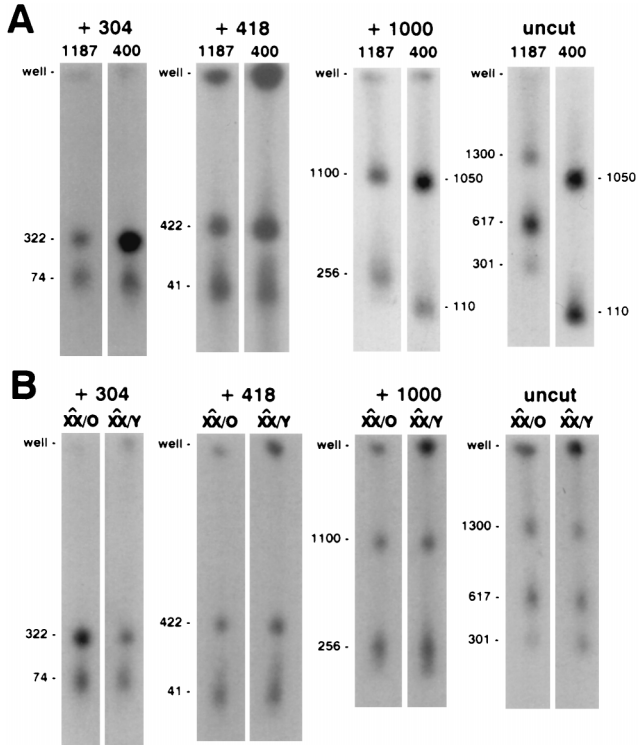

FIG. 5. The alteration of heterochromatic DNA structure is not correlated with PEV. (A) DNA was isolated from adult ovaries of flies containing either the *Dp1187* (lanes 1187) or the *Dp400* (lanes 400) chromosome and digested with *Mlu*I (+304), *Hpa*I (+418), or *Not*I (+1,000) or left undigested (uncut). The shortened heterochromatic DNAs contained in these samples were visualized by two-dimensional agarose gel hybridization as described for Fig. 3. Only the *Dp1187*-derived and *Dp400*-derived molecules are shown, to make comparison easier. *Dp1187* and *Dp400* samples for each digest were analyzed in parallel. A 10- to 150-s linearly ramped switch time was used for the first-dimension CHEF electrophoresis. The sizes (in kilobase pairs) of full-length and shortened molecules are indicated. (B) DNA was isolated from adult ovaries of flies of genotypes $X\hat{}X, y$/O; *Dp1187*, y^+ (lanes X^X/O) and $X\hat{}X, y/Y$; *Dp1187*, y^+ (lanes X^X/Y). The DNA was digested and the shortened heterochromatic DNAs were visualized as described for panel A.

ened DNA molecules detected in these digests (Fig. 5A). This result suggests that alterations to the structure of heterochromatic DNA encompassed by the +304 and +418 restriction fragments do not differ significantly between the *Dp400* and *Dp1187* chromosomes despite a significant difference in *yellow* variegation. The +304 and +418 restriction fragments encompass sequences from kb −18, which is 2 kb proximal of the euchromatic *yellow* gene, through 418 kb of heterochromatic sequences (Fig. 1).

If alterations of *Dp1187* structure cause *yellow* variegation, modifiers of variegation acting in *trans* would be expected to alter the sizes of the shortened *Dp1187* molecules. To test this hypothesis, *Dp1187* molecules of altered structure were characterized in flies in which *yellow* variegation was modified in *trans* by the *Y* chromosome rather than in *cis*, as was the case with the terminal deletion of *Dp400*. Female flies of genotypes $X\hat{}X, y$/O; *Dp1187*, y^+ and $X\hat{}X, y/Y$; *Dp1187*, y^+ in which the frequency of *yellow*$^-$ triple-row bristles was 42% and 3%, respectively, were generated (17). DNA molecules of altered structure were revealed in uncut and restriction enzyme-digested ovary DNA by two-dimensional electrophoresis, and the results are illustrated in Fig. 5B. No consistent differences were observed between the two genotypes in the shortened *Dp1187* molecules detected in +304, +418, +1,000, or uncut DNA samples, despite a greater-than-10-fold difference in *yellow* variegation (Fig. 5B). This result, along with the results of the +304 and +418 digests of *Dp400* (Fig. 5A), demonstrates that changes to *yellow* variegation do not always correlate with changes in *Dp1187* structure. Such a correlation might have been expected if *yellow* variegation were caused by heterochromatic underrepresentation or the changes in DNA structure that underrepresentation creates.

DISCUSSION

We have identified heterochromatic DNAs of altered structure in polyploid cells of *Drosophila*. Altered heterochromatic DNA was found in the polyploid cells of both the ovary and salivary gland and was formed within heterochromatic sequences of both the *Dp(1;f)1187* minichromosome and chromosome III. These results suggest that the structure of heterochromatic DNA is altered as a general consequence of polyploid chromosome formation and that the shortened molecules characterized in this report are the discontinuous DNA molecules predicted to form within underrepresented sequences.

Three different hypotheses have been proposed for the mechanism of underrepresentation: (i) heterochromatic sequences are underreplicated because replication forks that initiate within euchromatic sequences stall as they attempt to traverse heterochromatin (29); (ii) heterochromatic sequences are actively removed by a process of DNA elimination (27, 46); and (iii) replication of heterochromatic sequences is bypassed in a process of copy-choice replication, in which DNA polymerase switches templates during replication of repetitive sequences (21). Each mechanism predicts the formation of DNA molecules of altered structure within underrepresented heterochromatin. Different structures are predicted to form for each mechanism, specifically, (i) nested replication forks in the underreplication model (29), (ii) truncated and rearranged DNA molecules in the elimination model (46), (iii) molecules containing a network of excluded DNA loops in the copy-choice replication model (21). Determining if the shortened heterochromatic DNAs characterized in this report have any of these structures will show which of the proposed mechanisms causes heterochromatic underrepresentation.

The properties of the altered heterochromatic DNAs reported here are not consistent with the nested-fork structures predicted by the underreplication model. Altered *Dp1187* molecules appear to be shortened in size based on their increased electrophoretic mobility (Fig. 3 to 5), yet DNA molecules containing replication forks migrate larger than their linear counterpart, not smaller (4). In addition, the shortened heterochromatic molecules do not appear to contain replication forks, at least none that compose a large fraction of total molecule length, since they do not migrate in a manner characteristic of fork-containing molecules on appropriate two-dimensional gels (unpublished observation). An earlier analysis of *Dp1187* sequences that were underrepresented in salivary gland DNA also failed to identify fork-containing molecules (16). Finally, even if replication forks stall within a particular region of *Dp1187* but are subsequently broken in vivo or during DNA isolation, the stalled-replication model is still difficult to reconcile with the data reported here. Specifically, no common site or region of DNA breakage is apparent when the heterochromatic endpoints of the shortened *Dp1187* DNAs for different digests are mapped relative to the sc^8 breakpoint (Fig. 6). Even after accounting for size heterogeneity, the heterochromatic endpoints for different digests are significantly different (Fig. 6).

Both the elimination and copy-choice models of underrep-

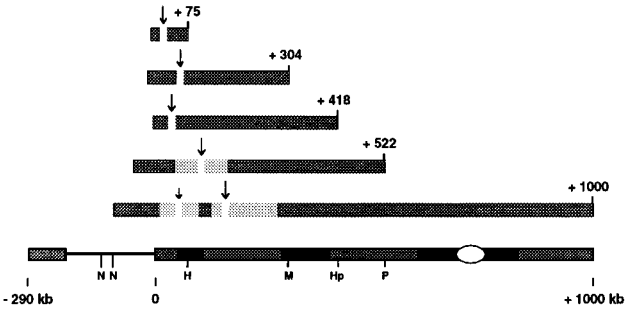

FIG. 6. Mapping the proximal endpoints of the shortened heterochromatic molecules does not reveal a common site of DNA breakage. Full-length restriction fragments are illustrated as gray bars above a map of the *Dp(1;f)1187* chromosome, and their normal proximal endpoints are indicated in kilobase pairs. The proximal endpoint of the most abundant shortened molecules observed for each digest is indicated by a vertical arrow and a gap in the full-length restriction fragment. The size of the gaps and the light gray areas for fragments +522 and +1,000 indicate the degree of size heterogeneity of the shortened molecules. The height of the vertical arrow indicates relative abundance. The proximal endpoints of the shortened molecules were mapped by assuming a linear DNA structure and simple DNA truncation within heterochromatic sequences (see Discussion). The structure and restriction sites of the *Dp1187* chromosome are as described for Fig. 1.

resentation provide a testable rationale for the observed differences in the heterochromatic endpoints of the shortened molecules (Fig. 6). For example, if DNA rearrangements accompany a process of heterochromatic elimination, as has been suggested (27, 46), new heterochromatic endpoints might arise as a consequence of newly positioned restriction sites. Heterogeneity in the sizes of shortened DNAs would result from imprecision in the rearrangement processes. If, on the other hand, copy-choice replication generates the shortened *Dp1187* molecules, these molecules might have a nonlinear structure that includes a network of DNA loops (21). Nonlinearity in DNA structure would be expected to affect the electrophoretic migration of the shortened molecules independently of their linear size and complicate the interpretation of the linear mapping approach illustrated in Fig. 6. Consistent with this possibility, the sizes of the shortened *Dp1187* molecules demonstrate sensitivity to parameters of electrophoresis. Specifically, increasing the temperature of electrophoresis causes increased heterogeneity in the sizes of the shortened molecules while having no effect on full-length heterochromatic or euchromatic control fragments (unpublished observation). This temperature sensitivity may indicate that the shortened heterochromatic molecules contain nonlinear structures. We are currently testing predictions of both the elimination and copy-choice models of underrepresentation to elucidate the structures of the altered heterochromatic molecules.

Changes in the variegated expression of the *yellow* gene were not consistently correlated with changes in *Dp1187* structure (Fig. 5), as might have been expected if *yellow* variegation were caused by changes in DNA copy number or structure. Since *yellow* variegation and *Dp1187* structure were assayed in different tissues, however, the data do not exclude the possibility that some instances of PEV are indeed caused by irreversible changes in the structure of DNA (27, 45). Nonetheless, our results are more concordant with a growing body of evidence indicating that most cases of PEV are caused by a reversible epigenetic mechanism (1, 8, 9, 20, 22, 34, 52).

The terminal deletion that forms *Dp400* caused both an increase in *yellow* variegation and unexpected changes in the structure of shortened derivatives of *Dp1187* (Fig. 5A, +1,000 and uncut samples) (45). If, as discussed above, *yellow* variegation is not a consequence of changes in DNA structure, the terminal deletion must affect both PEV and DNA structure independently. Large-scale looping interactions between different chromosome regions have been suggested to play a role in the mechanism of PEV and have been directly demonstrated in the case of the variegating *brown*^{D} gene (8, 9, 21, 42). Perhaps the terminal deletion alters such large-scale interactions, allowing conformations of the chromosome that increase *yellow* variegation. By the same mechanism, the terminal deletion might influence the structure of shortened derivatives of *Dp1187* if such large-scale interactions also play a role in heterochromatic underrepresentation.

Alteration of heterochromatic DNA structure in polyploid chromosomes of *Drosophila*, as illustrated in this report, provides yet another example of the dynamic character of heterochromatin. Determining the structure of the altered heterochromatic molecules will help elucidate the mechanism of heterochromatic underrepresentation and provide insights into how the genetic components of heterochromatin create the unique characteristics of this chromosomal domain.

ACKNOWLEDGMENTS

We are grateful to A. Spradling and P. Zhang for providing fly strains containing heterochromatic P-element insertions and to G. Karpen for providing fly strain *Df(1)sc*^{8}; *Dp1187*. We thank the anonymous reviewers for helpful comments. We acknowledge the Wadsworth Center Molecular Genetics Core Facility for assistance with CHEF electrophoresis.

This work was supported by Public Health Service grant GM53476-01 from the National Institute of General Medical Sciences and a grant from Health Research, Inc., both to R.L.G.

REFERENCES

1. **Ahmad, K., and K. G. Golic.** 1996. Somatic reversion of chromosomal position effects in Drosophila melanogaster. Genetics **144:**657–670.
2. **Baksa, K., H. Morawietz, V. Dombradi, M. Axton, H. Taubert, G. Szabo, I. Torok, A. Udvardy, H. Gyurkovics, B. Szoor, D. Glover, G. Reuter, and J. Gausz.** 1993. Mutations in the protein phosphatase 1 gene at 87B can differentially affect suppression of position-effect variegation and mitosis in *Drosophila melanogaster*. Genetics **135:**117–125.
3. **Beerman, S.** 1977. The diminution of heterochromatic chromosomal segments in Cyclops (Crustacea, Copepoda). Chromosoma **60:**297–344.
4. **Brewer, B. J., and W. L. Fangman.** 1987. The localization of replication origins on ARS plasmids in *S. cerevisiae*. Cell **51:**463–471.
5. **Chu, G., D. Vollrath, and R. W. Davis.** 1986. Separation of large DNA molecules by contour-clamped homogeneous electric fields. Science **234:** 1582–1585.
6. **Church, G., and W. Gilbert.** 1984. Genomic sequencing. Proc. Natl. Acad. Sci. USA **81:**1991–1995.
7. **Cleard, F., M. Matsarskaia, and P. Spierer.** 1995. The modifier of position-effect variegation Suvar(3)7 of *Drosophila*: there are two alternative transcripts and seven scattered zinc fingers, each preceded by a trypotophan box. Nucleic Acids Res. **23:**796–802.
8. **Csink, A. K., and S. Henikoff.** 1996. Genetic modification of heterochromatic association and nuclear organization in Drosophila. Nature **381:**529–531.
9. **Dernburg, A. F., K. W. Broman, J. C. Fung, W. F. Marshall, J. Philips, D. A. Agard, and J. W. Sedat.** 1996. Perturbation of nuclear architecture by long-distance chromosome interactions. Cell **85:**745–759.
10. **Dernburg, A. F., J. W. Sedat, and R. S. Hawley.** 1996. Direct evidence of a role for heterochromatin in meiotic chromosome segregation. Cell **86:**135–146.
11. **Elgin, S. C.** 1996. Heterochromatin and gene regulation in Drosophila. Curr. Opin. Genet. Dev. **6:**193–202.
12. **Feinberg, A. P., and B. Vogelstein.** 1983. A technique for radiolabelling DNA restriction endonuclease fragments to high specific activity. Anal. Biochem. **132:**6–13.
13. **Gall, J. G., E. H. Cohen, and M. L. Polan.** 1971. Repetitive DNA sequences in *Drosophila*. Chromosoma **33:**319–344.
14. **Garzino, V., A. Pereira, P. Laurenti, Y. Graba, R. W. Levis, P. Y. Le, and J. Pradel.** 1992. Cell lineage-specific expression of *modulo*, a dose-dependent modifier of variegation in *Drosophila*. EMBO J. **11:**4471–4779.
15. **Geyer-Duszynska, I.** 1959. Experimental research on chromosome elimination in *Cecidomyidiae* (Diptera). J. Exp. Zool. **141:**391–447.
16. **Glaser, R. L., G. H. Karpen, and A. C. Spradling.** 1992. Replication forks are

not found in a *Drosophila* minichromosome demonstrating a gradient of polytenization. Chromosoma **102:**15–19.
17. **Glaser, R. L., and A. C. Spradling.** 1994. Unusual properties of genomic DNA molecules spanning the euchromatic-heterochromatic junction of a Drosophila minichromosome. Nucleic Acids Res. **22:**5068–5075.
18. **Hammond, M. P., and C. D. Laird.** 1985. Chromosome structure and DNA replication in nurse and follicle cells of *Drosophila melanogaster*. Chromosoma **91:**267–278.
19. **Hammond, M. P., and C. D. Laird.** 1985. Control of DNA replication and spatial distribution of defined DNA sequences in salivary gland cells of *Drosophila melanogaster*. Chromosoma **91:**279–286.
20. **Henikoff, S.** 1979. Does position-effect variegation in Drosophila result from somatic gene loss? p. 123–132. *In* R. Axel, T. Maniatis, and C. F. Fox (ed.), Eucaryotic gene regulation. Academic Press, Inc., New York, N.Y.
21. **Henikoff, S.** A pairing-looping model for position-effect variegation in Drosophila. *In* J. P. Gustafson, and R. B. Flavell (ed.), Genomes: Proceedings of the 21st Stadler Genetics Symposium, in press. Plenum Press, New York, N.Y.
22. **Henikoff, S.** 1981. Position-effect variegation and chromosome structure of a heat shock puff in Drosophila. Chromosoma **83:**381–393.
23. **John, B.** 1988. The biology of heterochromatin, p. 1–147. *In* R. S. Verma (ed.), Heterochromatin: molecular and structural aspects. Cambridge University Press, Cambridge, United Kingdom.
24. **Karpen, G. H.** 1994. Position-effect variegation and the new biology of heterochromatin. Curr. Opin. Genet. Dev. **4:**281–291.
25. **Karpen, G. H., M.-H. Le, and H. Le.** 1996. Centric heterochromatin and the efficiency of achiasmate disjunction in *Drosophila* female meiosis. Science **273:**118–122.
26. **Karpen, G. H., and A. C. Spradling.** 1992. Analysis of subtelomeric heterochromatin in the *Drosophila* minichromosome *Dp1187* by single P element insertional mutagenesis. Genetics **132:**737–753.
27. **Karpen, G. H., and A. C. Spradling.** 1990. Reduced DNA polytenization of a minichromosome region undergoing position-effect variegation in *Drosophila*. Cell **63:**97–107.
28. **Kellum, R., and B. M. Alberts.** 1995. Heterochromatic protein 1 is required for correct chromosome segregation in Drosophila embryos. J. Cell Sci. **108:**1419–1431.
29. **Laird, C. D.** 1973. DNA of *Drosophila* chromosomes. Annu. Rev. Genet. **7:**177–204.
30. **Le, M.-H., D. Duricka, and G. H. Karpen.** 1995. Islands of complex DNA are widespread in Drosophila centric heterochromatin. Genetics **141:**283–303.
31. **Lindsley, D. L., and G. G. Zimm.** 1992. The genome of *Drosophila melanogaster*. Academic Press, Inc., New York, N.Y.
32. **Lohe, A. R., and A. J. Hilliker.** 1995. Return of the H-word (heterochromatin). Curr. Opin. Genet. Dev. **5:**746–755.
33. **Lohe, A. R., A. J. Hilliker, and P. A. Roberts.** 1993. Mapping simple repeated DNA sequences in heterochromatin of *Drosophila melanogaster*. Genetics **134:**1149–1174.
34. **Lu, B. Y., C. P. Bishop, and J. C. Eissenberg.** 1996. Developmental timing and tissue specificity of heterochromatin-mediated silencing. EMBO J. **15:** 1323–1332.
35. **Lyon, M. F.** 1961. Gene action in the X chromosome of the mouse (*Mus musculus*). Nature **190:**372–373.
36. **Madireddi, M. T., R. S. Coyne, J. F. Smothers, K. M. Mickey, M.-C. Yao, and C. D. Allis.** 1996. Pdd1p, a novel chromodomain-containing protein, links heterochromatin assembly and DNA elimination in Tetrahymena. Cell **87:** 75–84.
37. **Murphy, T. D., and G. H. Karpen.** 1995. Interactions between the nod$^+$ kinesin-like gene and extracentromeric sequences are required for transmission of a Drosophila minichromosome. Cell **81:**139–148.
38. **Murphy, T. D., and G. H. Karpen.** 1995. Localization of centromere function in a Drosophila minichromosome. Cell **82:**599–609.
39. **Nakai, Y., S. Kubota, Y. Goto, T. Ishibashi, W. Davidson, and S. Kohno.** 1995. Chromosome elimination in three Baltic, south Pacific and north-east Pacific hagfish species. Chromosome Res. **3:**321–330.
40. **Prescott, D. M.** 1992. Cutting, splicing, reordering, and elimination of DNA sequences in hypotrichous ciliates. Bioessays **14:**317–324.
41. **Rudkin, G. T.** 1969. Non-replicating DNA in *Drosophila*. Genetics **61:**227–238.
42. **Sabl, J. F., and S. Henikoff.** 1996. Copy number and orientation determine the susceptibility of a gene to silencing by nearby heterochromatin in Drosophila. Genetics **142:**447–458.
43. **Sambrook, J., E. F. Fritsch, and T. Maniatis.** 1989. Molecular cloning: a laboratory manual, 2nd ed. Cold Spring Harbor Laboratory Press, Cold Spring Harbor, N.Y.
44. **Smith, A. V., and T. L. Orr-Weaver.** 1991. The regulation of the cell cycle during *Drosophila* embryogenesis. Development **112:**997–1008.
45. **Spradling, A. C.** 1993. Position effect variegation and genomic instability. Cold Spring Harbor Symp. Quant. Biol. **58:**585–596.
46. **Spradling, A. C., G. Karpen, R. Glaser, and P. Zhang.** 1993. Evolutionary conservation of developmental mechanisms: DNA elimination in *Drosophila*. Symp. Soc. Dev. Biol. **50:**39–53.
47. **Spradling, A. C., and T. Orr-Weaver.** 1987. Regulation of DNA replication during Drosophila development. Annu. Rev. Genet. **21:**373–403.
48. **Tobler, H., A. Etter, and F. Muller.** 1992. Chromatin diminution in nematode development. Trends Genet. **8:**427–432.
49. **Tower, J., G. H. Karpen, N. Craig, and A. C. Spradling.** 1993. Preferential transposition of Drosophila P elements to nearby chromosomal sites. Genetics **133:**347–359.
50. **Truman, J. W., B. J. Taylor, and T. A. Awad.** 1993. Formation of the adult nervous system, p. 1245–1276. *In* M. Bate and A. Martinez Arias (ed.), The development of *Drosophila melanogaster*. Cold Spring Harbor Laboratory Press, Cold Spring Harbor, N.Y.
51. **Tschiersch, B., A. Hofmann, V. Krauss, R. Dorn, G. Korge, and G. Reuter.** 1994. The protein encoded by the *Drosophila* position-effect variegation suppressor gene *Su(var)3-9* combines domains of antagonistic regulators of homeotic gene complexes. EMBO J. **13:**3822–3831.
52. **Wallrath, L. L., V. P. Guntur, L. E. Rosman, and S. C. R. Elgin.** 1996. DNA representation of variegating heterochromatic *P* element inserts in diploid and polytene tissues of *Drosophila melanogaster*. Chromosoma **104:**519–527.
53. **Weiler, K., and B. Wakimoto.** 1995. Heterochromatin and gene expression in Drosophila. Annu. Rev. Genet. **29:**577–605.
54. **Zhang, P., and A. C. Spradling.** 1995. The Drosophila salivary gland chromocenter contains highly polytenized subdomains of mitotic heterochromatin. Genetics **139:**659–670.
55. **Zhang, P., and A. C. Spradling.** 1993. Efficient and dispersed local P element transposition from *Drosophila* females. Genetics **133:**361–373.
56. **Zhang, P., and A. C. Spradling.** 1994. Insertional mutagenesis of Drosophila heterochromatin with single P elements. Proc. Natl. Acad. Sci. USA **91:** 3539–3543.